

## TOPICAL REVIEW

# Noise and Vibration in Switched Reluctance Motors: A Review on Structural Materials, Vibration Dampers, Acoustic Impedance, and Noise Masking Methods

**ASHISH KUMAR SAHU**<sup>id</sup>, (Member, IEEE), **ALI EMADI**<sup>id</sup>, (Fellow, IEEE),  
**AND BERKER BILGIN**<sup>id</sup>, (Senior Member, IEEE)

McMaster Automotive Resource Centre (MARC), McMaster University, Hamilton, ON L8P 0A6, Canada

Corresponding author: Ashish Kumar Sahu (sahua1@mcmaster.ca)

This work was supported in part by the Natural Sciences and Engineering Research Council of Canada (NSERC), and in part by the Canada Excellence Research Chairs (CERC).

**ABSTRACT** Today, the majority of the commercial electrified vehicles use Interior Permanent Magnet Motors (IPMSMs) for propulsion. An IPMSM can deliver high starting torque and high efficiency in the low- and medium-speed operation, which makes it attractive for propulsion applications. However, IPMSMs generally utilize rare-earth permanent magnets and there are growing concerns about the price volatility and supply chain of these materials. Switched Reluctance Motors (SRMs) can potentially replace IPMSMs in various applications including propulsion. An SRM has a simple and low-cost construction, and it can provide reliable operation at high-speed and high-temperature conditions. Compared to IPMSMs, SRMs radiate considerably higher acoustic noise, which have historically hindered their widespread acceptance. Various approaches to mitigate acoustic noise and vibration at the source level have already been explored in the literature by improving the electromagnetic design and current control. This paper explores multiple noise and vibration mitigation methods that can be applied at the transmission stage. First, the noise comparison between the Internal Combustion Engine (ICE) and SRMs is discussed, and then the methods used for ICEs are presented for their applicability to SRMs.

**INDEX TERMS** Active noise control, active vibration control, noise and vibration, noise masking, sound absorber, sound barrier, switched reluctance motor, vibration damper, vibration isolator.

## I. INTRODUCTION

High starting torque, high power at high speed, high torque and power density, and higher efficiency over a wide speed range are some of the requirements for traction motors [1], [2]. Today, Interior Permanent Magnet Synchronous Motors (IPMSMs) are most commonly applied to propulsion applications because of their high power density and efficiency [2]. However, due to the increasing price volatility and supply chain issues of rare earth metals, there is a growing need for rare-earth-free motors, not only in electric

traction systems, but electric motor applications in general. Switched Reluctance Motors (SRMs) propose an alternative to IPMSMs. An SRM has simple and robust construction, and can operate at high-speed and high-temperature conditions. It can be designed to match the efficiency and performance of an IPMSM [3], [4], [5]. However, due to their double salient pole structure, SRMs are prone to relatively higher acoustic noise and vibration as compared to IPMSMs [6], [7].

Structure-borne noise due to the radial electromagnetic forces is usually the most prominent noise source in an SRM. There are various studies available in the literature on mitigation of the noise at the source level. However, limited studies are available for noise and vibration mitigation at

The associate editor coordinating the review of this manuscript and approving it for publication was Jingang Jiang<sup>id</sup>.

the transmission stage, while multiple methods are applied to Internal Combustion Engines (ICEs). When the noise is transmitted through a vibrating structure, it is called structure-borne noise, whereas when it is transmitted directly through the air, it is called airborne noise.

A comparison of electric motors, in general, to ICEs shows that electric motors are much quieter than ICEs [8], [9], [10]. This leads us to question why we are so concerned about electric motor noise. The reason lies in how we perceive the noise generated by an electric motor and an ICE. An ICE has multiple noise sources, leading to broadband noise comprising tonal, impulsive, and flow noises [11], [12]. Even though ICE noise has a tonal component, it is masked by impulsive and flow noises. On the other hand, electric motors generally have pure tonal electromagnetic noise at high frequencies, and a mix of tonal and broadband noise at low frequencies. This makes electric motor noise perceived as more annoying when compared to engine noise [13]. Another factor is the frequency range of the two sources. Electric motors generate tonal noise at frequencies that are higher than the noise frequencies of a typical ICE. Our hearing system perceives high frequency and tonal noise relatively more annoying [10], [14], [15].

There are two major ways to manage the perceived annoyance of electric motor noise at the transmission stage: attenuating the noise and vibration or generating broadband noise to mask it. The first approach reduces the loudness of noise; hence, reduces annoyance. The second method makes the noise more pleasant without reducing its loudness.

This paper presents the noise and vibration mitigation techniques that can be applied at the transmission stage. It first presents the current research available for SRMs for acoustic noise and vibration reduction. Then, it discusses the differences between ICE and electric motor noise. The paper draws inspiration from the methods applied to ICEs and discusses their applicability to SRMs. It investigates material segregation based on loss modulus and loss tangent, and various means to use them for vibration mitigation. Methods to mitigate noise in the acoustic medium by introducing acoustic impedance are also discussed. Both approaches are categorized as active and passive methods. Finally, the paper presents methods for noise masking.

## II. NOISE CHARACTERISTICS OF ICES AND ELECTRIC MOTORS

Noise generated by an electric motor and an ICE are perceived differently by our auditory system. Engines have multiple vibration sources, which lead to a wide range of noise frequencies [11]. Fuel combustion in the cylinder, which is the source of power generation, is the primary noise source. It leads to aerodynamic noise directly and also indirectly through crankcase vibration. The crank-train system transmits the force exerted by the piston to the output shaft through the crankshaft and flywheel. The valvetrain system and the cam drivetrain system, which includes the

camshaft, lever, and cams, open and close the air intake and exhaust valves. These mechanical devices have metal-to-metal contact, leading to structure-borne noise. Besides, the fuel delivery system and airflow system have high-pressure fuel pumps and valves, which cause both structure-borne noise and air-borne noise. Boosting systems such as turbochargers and superchargers that are present in the modern engines contribute to the noise. The accessories like belts, tensioners, idlers, alternator exhaust systems, and gear systems generate both structural and air-borne noise.

The noise generated by an engine is broadband noise. It is a mix of tonal noise components, impulsive noise components, and flow noise components [12]. Tonal noise is defined as the noise with high energy with a single frequency or a limited frequency range and it stands out from the background noise. In an engine, tonal noise is generated from sources like turbochargers, generators, or gears. Impulsive noise is a sudden rise of noise for a short period of time, followed by a decay. Impulsive noise can exhibit a broader frequency spectrum with concentration of the sound energy at various frequencies [16]. In an engine, impulsive noise is usually generated from combustion or injectors. Flow noise is the noise generated by turbulent fluid over a surface and it can have a broad frequency spectrum [17]. In an engine, flow noise is generated from airflow or fluid flow. In comparison, electric motor noise is dominated by electromagnetic forces at relatively higher frequencies and it has pure tonal characteristics [13]. In an electric motor, mechanical sources contribute to low-frequency broadband noise.

The noise characteristics of electric motors and ICEs have been measured considering they were used in similar size vehicles. In [8], a comparison has been conducted between a Citroen Berlingo Electric Vehicle (EV) and the same model vehicle with an ICE. In the same study, a Nissan Leaf EV was compared to a Volkswagen Golf ICE vehicle. The noise from the vehicle was measured by a microphone at 7.5 m away from the vehicle to assess how the noise could be perceived by a pedestrian, as per ISO 362 [18]. Also, it is reported that below 30 km/h, the EVs are 2-5 dB less noisy than the ICE vehicles at different driving conditions, such as acceleration, deceleration, and constant speed drive. Above 30 km/h, tire and road noise become dominant, and it becomes challenging to distinguish the noise level between the EVs and the ICE vehicles [8]. A similar observation was made in [9] between ICE and EV mode of a hybrid electric vehicle (HEV) when the noise was measured at 2 m away from the vehicle. For a bus, the noise level of an electric-drive bus is generally lower than a diesel-engine-powered bus [10].

Even though electric motors can be regarded as less noisy than ICEs in terms of sound level, their noise might be perceived as more annoying due to their high-frequency and tonal noise characteristics [19]. The perceived annoyance of tonal noise is related to the amplitude of the noise with respect to the background noise. There are various measures to identify the quality of a tonal noise. Tone-to-noise ratio

measures the level of the tone relative to the background noise. For a tonal noise to be distinctively perceived, its tone-to-noise ratio should be at least 8 dB at higher frequencies [13].

Even lower amplitude tonal noise at a relatively quiet background can be annoying like mosquito's whine. Prominence ratio is another sound quality metric. It compares the sound pressure level at the tonal frequency with the adjacent frequency band that masks the tone. For sounds with the same prominence ratio, the one with higher frequency content can be perceived more annoying as compared to the one with lower frequency content [15]. This can also help justify why electric motor noise is perceived more annoying when compared to ICE noise. For an ICE, the tonal noise is usually masked by the broadband noise from multiple sources and, hence, the ICE sound is perceived more tolerable than electric motor noise even though the sound level is generally higher.

### III. CURRENT METHODS APPLIED TO MITIGATE ACOUSTIC NOISE IN SRMs

#### A. SOURCES OF NOISE

There are multiple noise sources in an SRM as depicted in Fig. 1. In addition to electromagnetic sources, mechanical and aerodynamic sources cause noise and vibration in an electric motor. Radial and tangential electromagnetic forces, and switching of the power converter are electromagnetic noise sources. There can be multiple reasons of mechanical noise in an electric motor [3], [20]. Improper motor assembly and manufacturing defects may lead to misaligned or bent shafts resulting in vibration. Bearing defects like misalignment, imbalance, wear, and corrosion can also lead to vibration. Over time, fasteners can loosen in an electric motor leading to increase in vibration. The rotor and stator axis eccentricity can lead to electromagnetic and mechanical noise. Rotating air between stator and rotor causes aerodynamic noise perceived as acoustic noise. Hence, these electromagnetic and mechanical factors result in vibration in an electric motor, leading to structure-borne noise. The vibration energy is then transferred to the air surrounding the motor and it leads to acoustic noise.

#### B. NOISE CONTROL AT THE SOURCE

Radial electromagnetic forces contribute more significantly to acoustic noise in an SRM, as the stiffness of the stator-frame assembly is usually lower in the radial direction than the tangential direction. Hence, strong radial forces cause deformation in the radial direction on the stator located outside of the rotor [21], [22], [23], [24].

The radial force density,  $F_r$ , and the tangential force density,  $F_t$ , acting on a stator pole face are functions of radial flux density,  $B_r$ , and tangential flux density,  $B_t$ , as shown in (1) and (2). The radial and tangential flux densities are function of time,  $t$ , and the circumferential position of a stator,  $\alpha$ . The parameter  $\mu_0$  represents the permeability of air. The harmonics of the radial force component are the primary

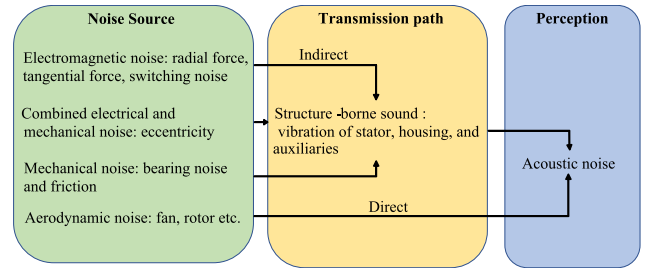


FIGURE 1. Typical vibration and noise sources in a switched reluctance motor.

reason for stator vibration, and the harmonics of tangential force component are the primary reason for torque ripple.

Noise and vibration mitigation at the source depends on the electric motor characteristics and its components. When targeting electromagnetic forces, either the harmonics of the tangential component or the harmonics of the radial component, the main methods for noise and vibration mitigation are typically enhancing the electromagnetic design or improving the current control [25]. Electromagnetic design can be improved by modifying the geometric structure of the rotor and stator assemblies. Typical improvements through current control involves optimization of control parameters, such as conduction angles and the shape of the phase current, within the given supply voltage limits. These approaches are at the source level. When developing these mitigation strategies, electric motor performance have to be considered.

$$F_r(t, \alpha) = \frac{1}{2\mu_0}(B_r^2(t, \alpha) - B_t^2(t, \alpha)). \quad (1)$$

$$F_t(t, \alpha) = \frac{1}{\mu_0}B_r^2(t, \alpha)B_t^2(t, \alpha). \quad (2)$$

Active vibration cancellation, current profiling, and direct instantaneous force control are the major source-level vibration reduction strategies in an SRM. In Active Vibration Control (AVC), a two-stage voltage excitation turn-off is applied with a constant zero-voltage period from the asymmetric bridge converter. It results in two oscillatory vibrations in opposite phases and reduces vibration [26], [27]. Various approaches have been opted to optimize the current profile using optimization strategies. An optimization algorithm is employed to eliminate the higher temporal order of radial force density by using Gaussian-shaped radial force [7]. Also, flattening the summation of radial forces has been studied in [28]. Direct Instantaneous Force Control (DIFC) has been employed to reduce the mode-0 related vibration by controlling the overall radial force [29]. A control structure that includes a force reference generator and a feedforward force controller has been used to apply the DIFC. A hybrid excitation has been proposed in [30], where the outgoing phase and a portion of the incoming phase are overlapped.

Control strategies to reduce the torque ripple can be segregated based on indirect and direct torque control [21]. Torque Sharing Function (TSF) is an indirect torque control

technique where the torque is regulated by controlling the phase current. TSFs can be classified as analytical, dynamic allocation, or numerically-optimized based on the torque distribution scheme [21]. An analytical function based flexible offline TSF has been investigated, which leads to lower torque ripple than linear, cubic and exponential TSF [31]. Current shaping based on genetic algorithm has been investigated to minimize torque ripple while maintaining low copper loss [32]. A new current reference generation strategy has been investigated to minimize torque ripple with a lower current tracking error [33]. Genetic algorithm based optimized current harmonics injection has been investigated to minimize the torque ripple [34]. Online TSF has been applied to reduce RMS torque ripple up to 70% compared to conventional TSFs [35].

Motor geometry parameters, such as pole arc angle, and notches on the rotor and/or stator pole can significantly impact torque ripple [36], [37], [38], [39]. Application of pole shoes and a non-uniform stator pole has also been studied for torque ripple reduction [40]. The influence of pole shoe shape, rotor pole arc angle, and stator pole height on the torque ripple has been investigated in [5]. Double stator SRMs have also been developed to reduce radial force [41].

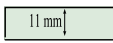
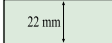

### C. NOISE CONTROL AT THE TRANSMISSION

Noise and vibration of an SRM can be improved either by improving the stiffness of the stator assembly or by increasing the damping of the structure. Increasing the stiffness of the stator assembly increases its natural frequency. Resonance is avoided if the natural frequency of the stator assembly is beyond the forcing frequency of the radial forces for the same circumferential mode. This reduces the stator frame deformation and, hence, helps mitigating acoustic noise. However, stiffness depends on the modulus of elasticity of the material and geometry of the structure. Stiffness should be increased with minimum increase in mass. Otherwise, it might impact the power and torque density of the motor. Introducing damping in the structure also helps reduce the amplitude of stator frame deformation during the resonance due to electromagnetic excitation.

Geometric improvements were investigated in the literature to increase the stiffness of the stator or the frame. Slot wedges have been used to improve the stiffness of an SRM stator [42], [43]. The effect of frame thickness and rib pattern has also been studied [44], [45]. The shape of the stator yoke design has been modified to improve the stiffness of the structure [46]. Also, damping material has been introduced to mitigate noise and vibration. A visco-elastic material can be used to encapsulate the windings and the properties are tuned to mitigate acoustic noise of an SRM [47].

It is evident from the available literature that most of the research for noise and vibration mitigation in SRMs focuses at the source. It is done mainly by geometric changes to improve the electromagnetic design or by enhancing the current control to improve the radial and tangential

**TABLE 1. Comparison of natural frequencies of a housing with and without ribs.**

Specification			
Mass (kg)	5.19	10.86	9.66
1 <sup>st</sup> Freq. (Hz)	6438	8207	8345
2 <sup>nd</sup> Freq. (Hz)	6503	8308	8460
3 <sup>rd</sup> Freq. (Hz)	6523	8318	8475

electromagnetic force variation. While some research shows efforts to improve the stiffness of the stator housing assembly, methods involving vibration damping materials and acoustic impedance need to be researched more.

### IV. STRUCTURAL DESIGN AND MATERIALS TO IMPROVE MODAL PERFORMANCE

At the transmission stage, the perceived annoyance from electric motor noise can be mitigated either by minimizing the loudness of the tonal noise with respect to background noise or by increasing the loudness of the background noise with respect to tonal noise. Reducing tonal noise loudness can be achieved mainly with two different methods. In the first method, structural vibrations can be minimized by improving damping in the structure or by shifting the natural frequency away from the excitation frequency. In the second method, the impedance of the acoustic waves in the acoustic medium are increased. These methods can be further classified as active and passive based on the energy required as input. Active methods need sensors, actuators, and control systems to operate. Passive methods rely on material properties.

Materials to attenuate structural damping can be categorized based on their loss modulus and loss tangent. Loss modulus is the product of loss tangent and dynamic shear modulus [20], [48]. The loss tangent, also referred to as the loss factor,  $\delta$  is the ratio of the imaginary to real part of the dynamic shear modulus. Hence, it is represented as  $\tan \delta$ . The imaginary part is a measure of the internal damping of the material and the real part is a measure of the stiffness of the material [3], [49].

In order to avoid excessive vibration, it is essential to keep the natural frequency of a component away from the excitation frequency. In an electric motor, the excitation frequency changes with the rotor speed; therefore, it is ideal to design the stator and housing assembly with natural frequencies as high as possible. This helps reduce the vibration due to excitation by radial forces because higher radial force harmonics usually do not have sufficient energy to excite the stator and housing assembly.

Natural frequency,  $f_n$ , depends on the structural stiffness to mass ratio,  $k/m$ , of the stator-housing assembly at different mode shapes, as shown in (3). Hence, structural stiffness to mass ratio is critical to mitigate noise in the transmission path. The structural stiffness of a component is a function of its

**TABLE 2.** Impact of different metals on the natural frequency.

Specification	Steel	Gray cast iron	Aluminum	Magnesium
Modulus of elasticity, E (GPa)	200	110	69	45
Density (kg/m <sup>3</sup> X 10 <sup>3</sup> )	7.8	7.2	2.7	1.7
Normalized natural frequency for the same thickness	1	0.75	1	1
Normalized natural frequency for the same weight	1	0.85	3.83	5.59
Normalized thickness of the cylindrical geometry for the same weight	1	1.07	2.07	4.08
Cost ( \$/MT in 2021-2022 )	800-1700	1500-1650	2500-2700	5000-6000
Thermal conductivity (W/mk)	45	53	237	157

shape and the modulus of elasticity of the material, which is calculated from the real part of the dynamic shear modulus. Table 1 compares the first three radial mode frequencies of a cylindrical housing with and without ribs. Adding ribs improves the stiffness-to-mass ratio more than the increase in thickness, which, in turn, lead to higher natural frequencies.

$$f_n = \frac{1}{2\pi} \sqrt{\frac{k}{m}} \quad (3)$$

Metals have high loss modulus, but low loss tangent. They are used in various engine parts, such as engine crankcase and engine cover. Table 2 compares the natural frequency of a hollow cylinder evaluated using finite element analysis for different metals. Metals such as steel, grey cast iron, aluminum, and magnesium are considered for the same hollow cylindrical geometry. The calculated natural frequencies are normalized to the natural frequency for steel.

For the same thickness, the natural frequencies for steel, magnesium, and aluminum are the same, because the ratio of the modulus of elasticity to mass density is the same for these materials. The natural frequency for grey cast iron is three-quarters of that of steel. A similar comparison is conducted for the same weight. As shown in Table 2, the natural frequencies for aluminum and magnesium are 3.83 and 5.59 times higher than steel, respectively, while their thickness is only 2.07 and 4.08 times larger than steel. This is one of the reasons why aluminum and magnesium are used in engine components like crankcase, engine cover, and front cover [50], [51], [52], [53]. Aluminum and grey cast iron alloys are also used for engine blocks and crankcase [54], [55]. Grey cast iron provides good damping capacity and temperature resistance. It is lighter than steel. Aluminum alloys have gained more popularity in engine applications due to their high strength-to-weight ratio, even though they are more expensive and have lower damping capacity. Magnesium

alloys have relatively higher damping capacity than steel, grey cast iron, or aluminum [20]. Even though magnesium is the lightest among these metals, it is not sufficiently stable at higher temperatures. Therefore, rather than the engine block, it is typically used for engine components such as front and top covers [11]. Recently, all-magnesium engine blocks have been developed using magnesium alloys that can withstand high temperatures [50], [51]. The temperature of an SRM housing is typically much lower than that of an engine. This makes magnesium a possible alternative to attenuate housing vibrations. One drawback of magnesium alloys is that their thermal conductivity is lower than aluminum alloys, which might impact the thermal management of the motor.

A material with a high loss modulus and a high loss tangent, such as composites, is ideal to mitigate structural vibration. The main benefit of composites is their higher strength and stiffness, and lower mass density. The properties of composites are usually anisotropic and can be tailored to the application requirements. Due to these benefits, carbon-fiber reinforced polymer has been used in the connecting rod and pistons of an engine [56]. Silicon Carbides (SiC) and glass carbon reinforced aluminum alloy has also been used in engine pistons [57], [58].

The loss factor of polymer matrix composites can be up to ten times higher than metals and alloys in the frequency range of 10-200 Hz [59]. The experimental loss factor of epoxy resin-based composites can increase as the frequency increases suggesting that composites can provide higher damping as compared to metals [60]. The damping of metals depends mainly on the hysteresis effect to dissipate the vibration energy. In composites, multiple factors contribute to energy dissipation, such as viscoelastic nature of the material and viscoplastic damping [61], [62]. Polymer matrix composites have high stiffness-to-weight ratio. Combined with its high loss factor, it can be a promising material to be used in the housing of an electric motor for vibration mitigation. However, polymer matrix composites usually have lower thermal conductivity than metals. A typical polymer matrix composite can have ten times lower conductivity than an aluminum alloy [63].

Metal matrix composites, such as SiC and aluminum alloy composites have higher thermal conductivity than aluminum alloys [64]. They also have a high stiffness-to-weight ratio. However, metal matrix composites show limited or marginal improvement in loss factor as compared to metals [65]. Therefore, they do not provide much improvement in structural damping. Metal matrix composites also have high production cost [66].

## V. PASSIVE DAMPING METHODS FOR VIBRATION ATTENUATION AT TRANSMISSION STAGE

Visco-Elastic Materials (VEMs) like natural rubber, neoprene and polymer rubbers have low loss modulus and high loss tangent. They are passive damping materials applied to improve damping if vibration attenuation due to structural

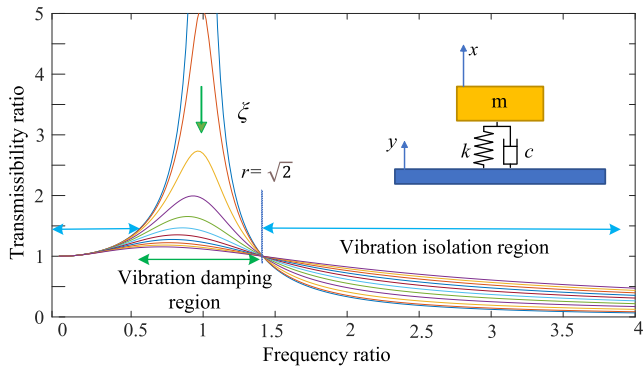


**FIGURE 2.** Transmissibility ratio of a mass excited by a base with sinusoidal excitation.

design is insufficient. Passive dampers are classified as vibration dampers or vibration isolators based on the transmissibility ratio required by the application. Fig. 2 shows the transmissibility plot for a mass excited by a base with sinusoidal excitation. The transmissibility ratio,  $TR$  is defined as the displacement of the mass,  $x$  with respect to the displacement of the base,  $y$  as shown in (4). It is a function of the ratio of the excitation frequency to the natural frequency,  $r$ , and damping ratio,  $\zeta$ . The damping ratio is a function of the mass, the stiffness and damping constant, which are dependent on the properties of the damping material. Vibration dampers dissipate the vibration energy as heat and reduce the vibration amplitude. On the other hand, vibration isolators shift the system’s natural frequency away from the excitation frequency by modifying the stiffness of the joint between the mass and the base. A frequency ratio above  $\sqrt{2}$  is ideal for vibration isolation because the transmissibility ratio would be less than one. In many applications, the frequency ratio is kept at a value where the transmissibility ratio is greater than one, but significantly lower than the transmissibility ratio of the damping region.

$$TR = \frac{x}{y} = \frac{\sqrt{(1 + (2r\zeta)^2)}}{\sqrt{((1 - r^2) + (2r\zeta)^2)}}. \quad (4)$$

A gasket is a vibration damper applied in ICEs [67], [68]. It is a thick, soft layer of rubber applied between the engine crankcase and cover to avoid metal-to-metal contact. Vibration dampers are also applied where the fuel rail is connected to the cylinder head and the transmission is connected to the engine block [69]. Vibration dampers with a smaller cross section applied axially between the stator poles and housing can reduce the radial acceleration of the housing surface by 10 folds [70]. Poor thermal conductivity of VEMs should also be considered when they are applied between the stator and housing for vibration damping [71]. Vibration isolators are applied as engine and exhaust mounts to isolate the vehicle chassis from the engine and exhaust vibrations [72], [73]. Fig. 3(a) and (b) show typical engine and exhaust mount constructions, where rubber is used at the joint to reduce the stiffness.

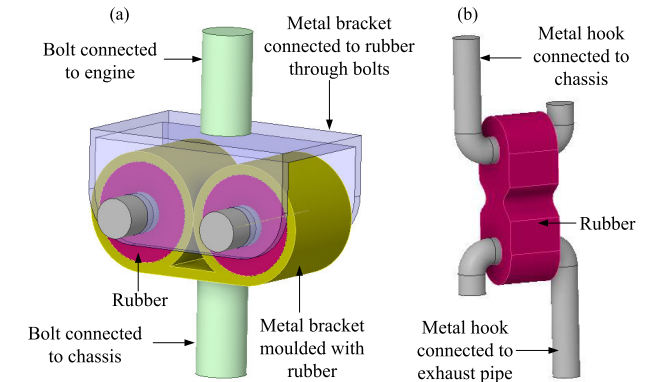


**FIGURE 3.** Vibration isolators: (a) engine mount, (b) exhaust mount.

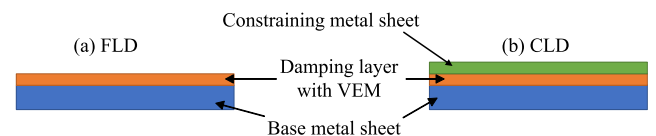


**FIGURE 4.** Use of viscoelastic materials for vibration damping: (a) Free layer damper, (b) constrained layer damper.

When viscoelastic materials are applied on metal surfaces to reduce vibration as shown in Fig. 4(a), it is referred as Free Layer Damping (FLD) [74]. FLD is suitable for thin panels such as a sheet metal oil sump [75]. Constrained Layer Damping (CLD), which consists of an additional layer of metal on top of the VEM as shown in Fig. 4(b), is more suitable for thicker panels. CLDs can provide significant vibration reduction and they were applied to an engine front cover [52], [76], a cast oil-pan [53], and a generator set cooling fan cover [77]. The observed damping effect is maximum when the constraining layer’s thickness is equal to the base layer [78]. Besides, the loss factor increases with a lower damping layer thickness [79]. Loss factor of a VEM improves in an FLD due to VEM bending deformation, and it is improved in a CLD due to VEM bending and shear deformation.

VEMs are also used as Tuned Mass Dampers (TMDs). TMD has been applied as torsional vibration dampers to mitigate crankshaft vibration [80]. Fig. 5 (a) shows a typical crankshaft torsional vibration damper. The rubber coupling between the inner and outer hubs acts as a damper. The secondary mass, and the rubber attached to the secondary mass to tune it act as a TMD. TMD has been applied to reduce cabin noise due to roof vibration [81]. It has also been applied to the transmission mount to reduce the noise and vibration of the vehicle [82]. Application of TMD on the suspension has also been investigated to reduce the car body vibration due to tire mass [83]. Fig. 5 (b) shows a tuned mass damper inside a suspension. The tuned mass slides on the strut and it is supported by spring and rubber damper on either sides. TMDs are more common in tall buildings like the Canadian National (C.N.) tower in Canada, Taipei 101 in Taiwan, and Citycorps

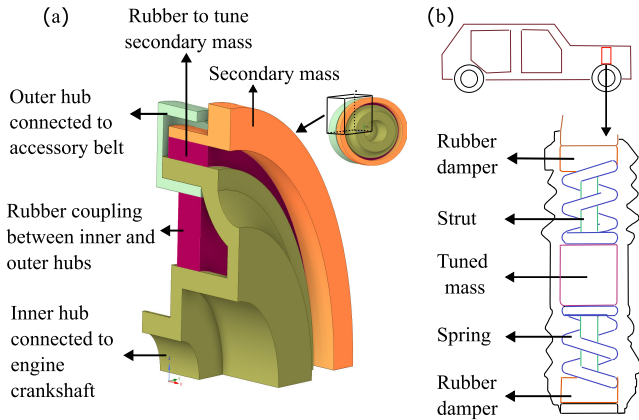


FIGURE 5. Examples of tuned mass dampers: (a) crankshaft torsional vibration damper, (b) suspension tuned mass damper.

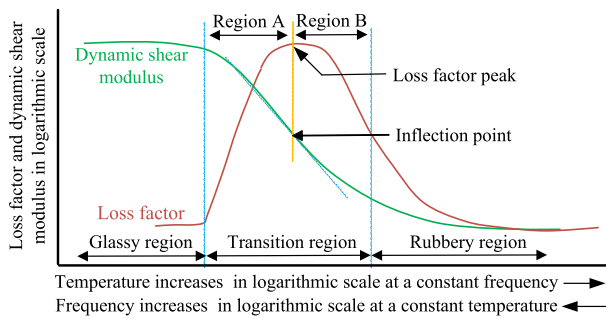


FIGURE 6. Representation of the effect of temperature and frequency on the dynamic shear modulus and loss factor for a typical viscoelastic material.

center in the USA [84], [85], [86]. TMDs are usually effective if only one vibration mode is dominant [87].

The loss factor of a VEM is strongly dependent on temperature and excitation frequency [88]. A log-log scale loss factor relationship with temperature and frequency specifies its application range [49], [89]. Fig. 6 shows the impact of temperature and frequency on the dynamic shear modulus and loss factor of a typical VEM. Dynamic shear modulus is the highest in the glassy region at low temperature. It reduces in orders of magnitude in the transition region as the temperature increases and it is the lowest in the rubbery region. The trend is reversed with an increase in frequency at a constant temperature. The loss factor has at least one peak, coinciding with the inflection point of the dynamic shear modulus in the transition stage. As depicted in Fig. 6, the transition region can be further divided into Region A and Region B [90]. The high dynamic shear modulus and high loss factor in Region A are suitable for FLDs. The lower dynamic shear modulus and a high loss factor in Region B are more suitable for CLDs. Low dynamic shear modulus and low loss factor make the rubbery stage suitable for tuned mass dampers. All other damping applications lie either in Region A or B [90]. The width and peak of loss factor depend both on the temperature and frequency [90], [91].

VEMs are efficient in wide frequency range but are applicable in a reasonably low-temperature range [47], [73]. VEMs can age due to oxidation [92]. The aging rate of VEMs increases with the time they are exposed to oxidation, the load cycle, and operating conditions such as high temperature, high shear load, and high frequency [73], [92], [93].

### VI. PASSIVE IMPEDANCE METHODS USING ACOUSTICAL MATERIALS FOR ACOUSTIC NOISE MITIGATION AT TRANSMISSION STAGE

Acoustic noise can be mitigated at the transmission stage by creating impedance in the acoustic medium. Acoustical materials such as sound absorbers or sound barriers are used for this purpose and they reduce the loudness of the noise. When it comes to material properties, loss modulus and loss tangent are not relevant any longer for acoustical materials. The effectiveness of a sound absorber is quantified by its absorption coefficient, which is defined as the ratio of the absorbed sound pressure to the incident sound pressure. For sound barriers, the effectiveness is quantified by their transmission coefficient, which is defined as the ratio of the transmitted sound energy to incident sound energy.

#### A. SOUND ABSORBERS

Sound-absorbing materials can be categorized as resonant absorbers and porous absorbers. Resonant absorbers operate based on the Helmholtz principle [94]. They consist of many cavities where the waves get trapped, resonate, and dissipate their energy. Resonant sound absorbers are typically more suitable at low frequencies, provide strong attenuation at critical frequencies but have a narrow bandwidth. Porous absorbers have a large number of interconnected small pores like a foam, which is effective in abetting acoustic noise in the mid- and high-frequency range [95], [96]. Sound absorbers have been applied on the dash panel and under the bonnet of ICE vehicles to mitigate engine noise and tire noise [97], [98]. 1-5 dB noise reduction was achieved by encapsulating the engine with a structural fiber and polyurethane foam, and by adding an underbody carpet made of a dense fiber acoustical layer [99]. A similar noise absorbing approach was applied to an electric vehicle [100].

Deterministic and semi-empirical models have been used to estimate acoustic noise reduction of a porous material [101], [102]. Equation (5) shows a model of acoustic damping considering porosity,  $\rho$ , flow resistivity,  $r$ , and tortuosity,  $s$ , of a porous material to model the sensitivity of sound absorption to frequency [103]. The variables  $p$ ,  $t$ , and  $x$  represent sound pressure, time, and position of a sound wave, respectively. Porosity is the ratio of the volume of voids to the volume of the entire structure. Flow resistivity is the ratio of a pressure gradient to flow velocity. Tortuosity defines the complexity of the porous structure. It was shown that the absorption coefficient is low at lower frequencies and significantly higher at higher frequencies if the thickness of the porous material is at least a quarter of the wavelength.

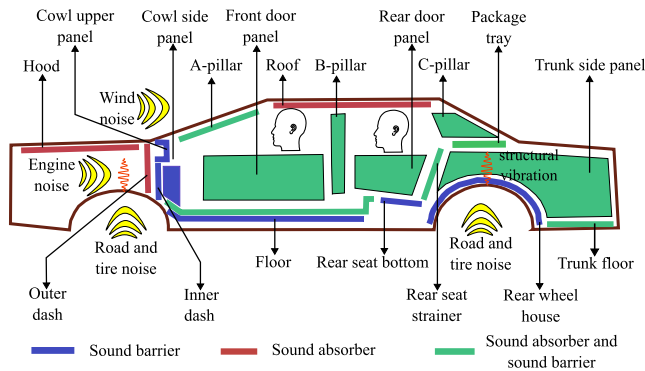


**FIGURE 7. Acoustical materials applied in a vehicle at different locations to attenuate engine, tire, road, wind, and panel vibration noise inside the cabin.**

An optimum value of flow resistivity and thickness in a sound absorber provides the best acoustic damping performance.

$$\frac{d^2p}{dx^2} = \frac{s}{c_0} \frac{d^2p}{dt^2} + \frac{rh}{c_0^2 \rho_0} \frac{dp}{dt}. \quad (5)$$

A porous material dissipates sound energy to heat energy through multiple ways such as: (i) frictional contact between the acoustic waves and the pores, (ii) heat conduction through pores, and (iii) vibration of the solid skeleton [103]. The effect of temperature on the acoustic property of sound absorbers has been studied in [104] and [105] up to 500°C. The acoustic speed and viscosity of air increase with an increase in temperature, leading to a shift of the acoustic absorption coefficient curve to higher frequency.

## B. SOUND BARRIERS

Sound barriers are materials that do not allow noise to pass through. They can be solid materials like metal, glass, polycarbonate, or acoustical materials such as loaded vinyl and loaded rubber [106]. Loaded means dense filler material that makes up the mass to reflect noise. Polymers like Polyvinyl Chloride (PVC) and Ethylene Vinyl Acetate (EVA) keep a noise barrier flexible. The transmission coefficient of sound barriers depends on the material's porosity, density, and limpness [106]. Holes in the material allow the energy to transmit, increasing its transmission coefficient. A limp structure does not transmit its own vibration energy and is suitable to be wrapped around curved vibrating surfaces. Density applies resistance to sound energy, reducing its transmission coefficient. Mass-loaded vinyl can be used on a dash panel, floor, and wheelhouse to insulate the cabin from the road and engine noise [107].

Sound barriers are primarily used in combination with sound absorbers. Noise barriers made of sound absorbers and barriers have been applied outdoors to mitigate traffic and industrial noise [108]. As shown in Fig. 7, sound barriers and sound absorbers can be used to mitigate acoustic noise inside a car cabin. There are multiple sources of noise in a car, such as an engine noise, road and tire noise, wind noise, and noise due to the structural vibration of body parts.

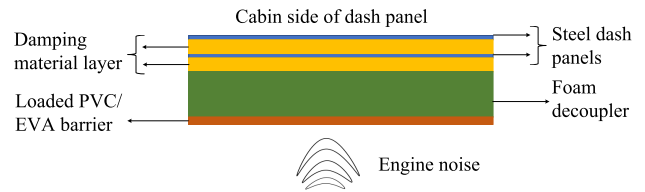


**FIGURE 8. Nissan Micra dash panel sound barrier assembly.**

Sound barriers and sound absorbers can be used standalone or in combination with each other to reduce the transmission coefficient of body panels. They can be applied to different vehicle body panels such as floor, roof, hood, and cowl [109]. They are either mounted with fasteners or pasted with adhesives to the body panels. Loaded PVC/EVA and a noise absorber have been used as a sandwich structure to form the Nissan Micra dash panel sound barrier assembly, as shown in Fig. 8 [110]. Bituminous damping material is inserted between the sheet metals to dampen their vibration, and foam is applied to decouple the sound barrier and sheet metal vibration. The double-walled construction of such barriers provides lower transmission coefficient than a single-wall construction of the same weight [109].

The transmission coefficient of a sandwich structure reduces with an increase in sound barrier's mass and decreases with an increase in frequency [111]. 1-4 dB noise reduction has been achieved by encapsulating an electric motor with a sound absorber and sound barrier combination. The maximum noise attenuation is observed at 10 kHz [112]. The efficiency of an encapsulation with a sound absorber and a sound barrier depends on how well the encapsulation covers the noise source [113]. Below 80% coverage, the performance of an encapsulation is driven by the absorption capacity of the material. Above 80%, it is driven by the transmission coefficient of the material.

## VII. ACTIVE AND SEMI-ACTIVE CONTROL METHODS TO MITIGATE NOISE AND VIBRATION AT THE TRANSMISSION STAGE

Passive damping techniques are effective over a broad range of frequencies; however, they are less effective or tend to become a bulky solution at lower frequencies. Active damping techniques such as Active Noise Cancellation (ANC) or Active Vibration Control (AVC) are more effective in attenuating low-frequency noise and vibration [114], [115]. In many applications, active and passive control techniques are used together to attenuate vibration and damping over a broad range of frequencies. VEMs are used with active or semi-active engine mounts and acoustic absorbers and barriers with ANCs for automotive applications. Active damping methods require sensors, actuators, and an external power source to operate. Semi-active damping techniques are an intermediate solution between passive and active damping techniques. In semi-active damping, the vibration-absorbing properties of the damper change with external vibration.



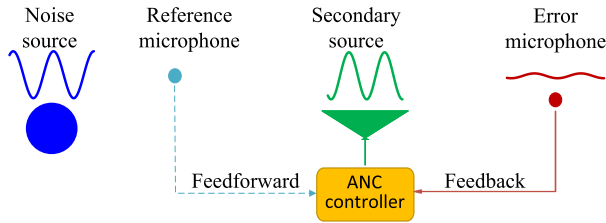


**FIGURE 9. Block diagram of feedback and feedforward control system mechanism for active noise cancellation.**

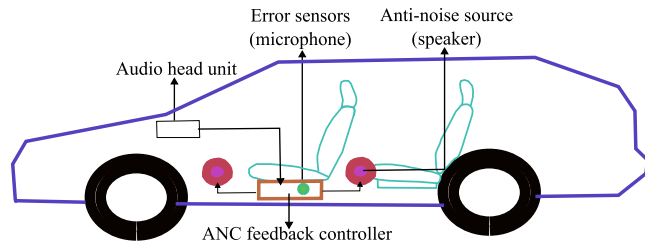


**FIGURE 10. Application of a feedback control active noise cancellation system in a vehicle.**

**A. ACTIVE NOISE CANCELLATION**

Active Noise Cancellation (ANC) functions on the principle of superposition. Noise generated by an external source is unwanted sound, and anti-noise is the sound generated by an electroacoustic device that cancels the noise. The anti-noise generated by the electroacoustic device is equal in magnitude and opposite in phase to the noise, resulting in noise cancellation. Theoretically, the resultant noise should be zero due to the superposition of noise and anti-noise, but some residual noise is always present due to practical challenges [116]. The effectiveness of an ANC system depends on the accuracy of the anti-noise generated by its control system.

As shown in Fig. 9, an ANC system uses a microphone as an error sensor to measure the resultant noise and provide feedback to the controller. A speaker is used as a secondary sound source to produce the anti-noise based on the controller input. The performance of the feedback system depends on the system delay, which might lead instability as the frequency increases. Therefore, ANC control bandwidth is inversely proportional to the distance between the error sensor and the anti-noise source [117]. Honda proposed a feedback ANC system to attenuate the cabin noise at 40 Hz, as shown in Fig. 10 [118]. Four speakers were used, one at each door, which were integrated with the music system, and the microphone was placed below the seat with the controller unit. A 10 dB noise reduction was observed. A feedback control system has also been proposed for headphones [119] and duct systems [120].

Active noise cancellation can also be configured with a feedforward control system as depicted with dashed lines in Fig. 9. It requires an additional microphone to measure the reference noise. Thus, the controller has the information on the noise before the noise reaches the error sensor through the

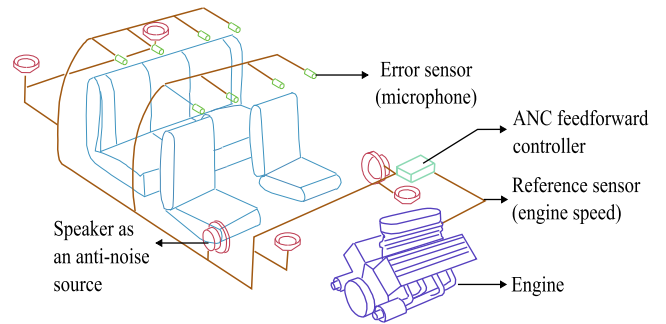


**FIGURE 11. Application of feedforward control active noise cancellation system.**

feedback signal. Coherence between the reference sensor and noise source is critical for the performance of the feedforward controller. Therefore, the reference sensor should be closer to the noise source for effective performance of feedforward controller [117], [121]. Casuality constraint is also critical for the performance of a feedforward controller. This sets a requirement for the minimum distance between the reference sensor and the anti-noise source [122]. The feedforward control system becomes unstable if the electrical delay is larger than the acoustic delay. The electrical delay includes the delays by adaptive filters, Analog-to-Digital (A/D) converters, Digital-to-Analog (D/A) converters, reconstruction filter, and the processing time of the controller. The acoustic delay is the time required for the noise from the reference sensor to reach the anti-noise source. A random broadband reference signal requires continuous tracking, and if the processing time is long, it may lead to a non-casual controller response and a substantially degraded performance. In a harmonic or narrow band noise, the reference signal can be easily predicted, so continuous tracking of the reference signal and casuality constraint requirements can be easily met [117], [121].

Feedforward ANC has been used to reduce 7 dB broadband noise in the frequency range between 100-200 Hz inside a vehicle cabin [123]. Six accelerometers were mounted on the suspension as reference sensors, two microphones were placed in the front headrest as error sensors, and two speakers were mounted on the front door as the anti-noise source. Feedforward ANC has also been applied to the exhaust muffler to attenuate low-frequency broadband noise between 100-700 Hz [115]. A microphone was placed close to the engine exhaust outlet, and a speaker was placed downstream of the duct. A 2-4 dB noise attenuation in the entire frequency band and a 10 dB attenuation at the peak noise frequencies were achieved. Fig. 11 shows a feedforward ANC applied to mitigate narrowband engine noise [124]. The reference signal was derived from the engine. Six speakers were used as anti-noise sources and eight microphones were placed on the roof as error sensors. A 10 dB noise attenuation was observed at 100 Hz and 4-5 dB in the entire frequency band.

Automotive ANC applications can also be categorized as global and local [123], [125]. A global approach requires multiple microphones and speakers positioned away from the listener to attenuate noise inside the cabin. The performance of a global approach can be improved by increasing the number of microphones and speakers, but its feasibility still depends on the size of the enclosure not being significantly larger than the acoustic wavelength [121]. Typically above 300 Hz, cabin acoustic modes overlap, limiting the speaker's ability to attenuate one mode without amplifying others [121], [126].

A local approach requires microphones and speakers to be placed close to the listener to create a zone-of-quietness around them. This approach provides a higher frequency limit than the global approach [125], [127]. The zone-of-quietness is the area where a 10 dB noise reduction can be achieved. For a single anti-noise speaker, the zone-of-quietness around an error sensor is limited to a diameter of about one-tenth of the acoustic wavelength [128]. By having four anti-noise speakers, the diameter of zone-of-quietness around the error sensor can be extended to six-tenth of the wavelength [127].

### B. ACTIVE AND SEMI-ACTIVE VIBRATION CONTROL

Active and semi-active vibration control systems work on the principle of superposition, similar to ANCs. Sensors such as load cells, accelerometers, or displacement transducers are used to measure error and reference signals. Piezoelectric, magnetostrictive, or electromagnetic actuators are used as secondary vibration sources [124], [129]. Both feedback and feedforward control has been applied in the literature for active and semi-active vibration control mechanisms [129]. Typically below 20 Hz, the engine mount requires high stiffness and high damping to resist the weight of the stationary engine. Above 20 Hz, in the engine running frequency range, the engine mount requires low stiffness and high damping for vibration isolation. Passive damping measures such as VEM cannot meet both requirements [130]. So an active or semi-active engine mounts have been used to address this issue.

Fig. 12 (a) shows a typical active engine mount system applied to mitigate second-order engine vibration at idle below 20 Hz [131]. It uses a multi-layer piezoelectric actuator. A viscous fluid chamber has been used to amplify the displacement output of the multi-layer piezoelectric actuator. Rubber, as a passive damping element has been used to withstand the engine mass and act as a failsafe measure in case of an actuator failure [130]. A piezoelectric engine mount has also been applied in Audi S8 to mitigate second- and fourth-order engine vibration between 25-250 Hz [132]. The crankshaft position has been used as a reference signal in this case. Electromagnetic actuators have also been used to develop active engine mounts [133]. On average, 5 dB noise reduction below 500 Hz was observed, when measured at the driver's position inside the cabin.

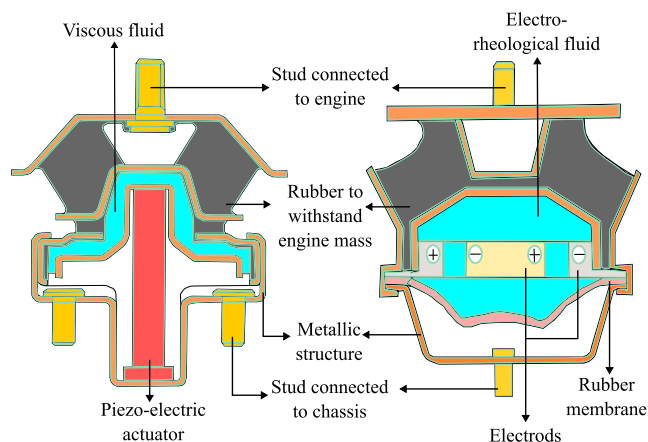


**FIGURE 12. Example of an active and a semi-active vibration control: (a) piezo-electric actuator based active engine mount, (b) electro-rheological fluid based semi-active engine mount.**

Fig. 12 (b) shows an Electro-Rheological (ER) fluid-based semi-active engine mount system [134]. ER fluid changes its viscosity based on the electric field applied through the electrodes in the lower chamber. This mechanism is used as the secondary vibration source against the engine vibration. ER fluid-based semi-active engine mount system has also been applied to achieve a ten-fold reduction in transmissibility ratio at 4.25 Hz [135]. A significant reduction in vibration was achieved at the driver's position below 30 Hz using a semi-active Magneto-Rheological (MR) engine mount system [136]. MR fluid changes its viscosity based on the applied magnetic field. The response time of all these active and semi-active actuators are typically a few milliseconds or more, which limits their operational frequency below 1 kHz [131], [137], [138], [139], [140]. These systems are generally placed only in the dominant vibration transfer path owing to the expensive actuators [124].

### VIII. ACTIVE SOUND DESIGN TO MASK THE TONAL NOISE OF AN ELECTRIC MOTOR

The annoyance associated with the acoustic noise of an electric motor can also be attenuated by artificially generating masking noise. Active Sound Design (ASD) is a methodology to design sound that can be played in a vehicle to improve interior sound quality and external sound to ensure pedestrian safety [141]. Traditionally ASD has been used to enhance the ICE vehicle noise and make it sound more pleasant and powerful, explicitly maintaining the brand image [142].

An electric vehicle might have the following sound-related issues to be addressed: (i) inadequate auditory response to dynamic driving conditions inside the cabin, (ii) insufficient external sound to alert pedestrians, and (iii) inadequate sound quality to match the brand image of automotive companies. In European regulations, an Acoustic Vehicle Alerting System (AVAC) for pedestrian safety requires a minimum of 50 dB(A) and 56 dB(A) sound level for a constant speed test at 10km/hr and 20km/hr, respectively [143]. Also, it requires

that the maximum level of sound for AVAC to be less than 75 dB(A) for M1 and N1 category vehicles when measured at a distance of 2 m, similar to sound level requirements for ICE vehicles [143], [144]. A vehicle for carrying passengers, comprising not more than eight seats excluding the driver's and having at least four wheels, is categorized as M1 by United Nations Economic Commission for Europe (UNECE). A vehicle carrying goods with a total mass of less than 3.5 tonnes and at least four wheels is categorized as N1 by UNECE. The regulation defines the minimum and maximum sound level but does not define the sound characteristics.

Designing a pleasant sound for an electric vehicle using an ASD can be challenging because it requires optimization of a combination of different noise harmonics [142]. Addition of a random broadband noise may increase the overall loudness. On the other hand, addition of a random narrowband noise may increase sharpness [145]. Sharpness is a psychoacoustic sound quality metric that compares high-frequency energy levels to the total energy. So, musical harmonic theory can be applied to identify the correct harmonics that need to be added to make the noise more pleasant [146]. Sound design for an electric vehicle is a relatively new issue for the automotive industry, so customer expectations are not defined yet due to the subjective nature of sound quality perception [145], [147], [148]. The inability of the conventional psychoacoustic noise metrics to differentiate all noises adds to the challenge [146].

Ricardo used ASD to generate an augmented interior sound for an electric vehicle [148]. An accelerometer mounted in an electric motor housing was used as a sensor. The signal's harmonic content was improved by frequency modulation, filtering, and audio effects depending on the vehicle speed and acceleration demand, which was then played through loudspeakers in the cabin. Mercedes have also developed an augmented sound system to provide tailor-made driving sound for different driving conditions [149].

## IX. COMPARISON AND DISCUSSIONS

Fig. 13 categorizes the methods investigated in this paper for acoustic noise and vibration mitigation at the transmission stage. Implementation of these methods depends on various factors, such the operating temperature, frequency range, and the impact of the method on the electromagnetic and thermal performance of the motor. Besides, cost, manufacturability, and compactness are critical factors to consider for commercial applications. Table 3 summarizes the advantages, challenges, possible application opportunities, and the estimated cost for the presented methods. For the cost estimation, a 24/16 SRM is considered with an outer diameter of 286 mm, axial length of 90 mm, and eight mounting location [4]. For the cost estimation, only the critical components and raw materials are considered.

### A. STRUCTURAL DESIGN AND MATERIALS

Improving the modal performance through structural design and materials can be preferred over active and passive

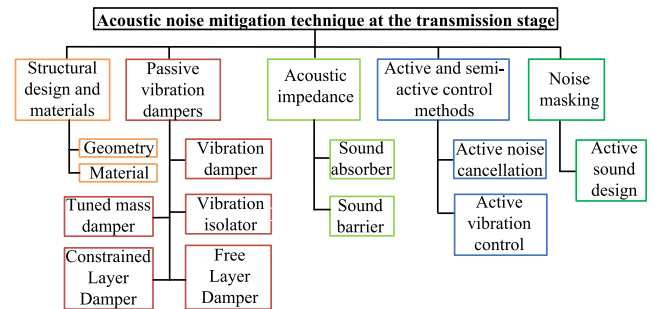


FIGURE 13. Acoustic noise mitigation techniques at the transmission stage discussed in this paper.

vibration and acoustic noise mitigation methods because it can be more effective, economical, and easier to implement. A stiffer structural housing and endplate geometry, combined with lower-mass-density and high-elastic-modulus material, is critical to improve the natural frequency of the stator housing assembly. A thicker housing and rib design can be utilized to improve the modal frequencies of the stator-housing assembly. Radial and screw type ribs can be more beneficial than axial ribs on the housing [44]. In Table 3, the housing and end plate thicknesses of the 24/16 SRM are considered as 11-22 mm and 2-4 mm, respectively, to estimate the cost of structural design. The weight of the housing and endplates are maintained the same for different materials. The cost estimate is based on the weight of the structure and material costs presented in Table 2.

### B. PASSIVE VIBRATION DAMPERS

Visco-Elastic Materials (VEMs) can be economical and various grades of VEM cater to a wide range of frequency requirements [150]. VEMs can be applied between the stator and housing [70] and between the housing and endcaps as vibration dampers. Free Layer Dampers (FLDs) can be applied to the endcaps as they are relatively thinner than the housing. Constrained Layer Dampers (CLDs) can be applied to the outer surface of the housing. These applications must be investigated considering the thermal performance of the motor, as VEMs can have low thermal conductivity [71]. VEMs can also be applied as vibration isolators at the mounting location of the motor. Tuned Mass Dampers (TMDs) are suitable for mitigating vibration for a dominant mode at a particular frequency. However, it is a challenge that electric motors can have resonance at multiple frequencies as the excitation frequency varies with speed.

It is assumed that a 5 mm thick VEM is applied as a vibration damper on ten percent of the circumferential area between the stator and housing, and a hundred percent of the area between housing and endplates. The estimated cost of the vibration damper is based on the weight of VEM applied on the 24/16 SRM. The outer surface area of end plates and housing is considered to estimate the cost of FLD and

**TABLE 3. Advantages, challenges, approximate cost estimation and possible application of acoustic noise and vibration mitigation methods for switched reluctance motors.**

Methods	Advantages	Challenges	Estimated Cost	Possible application in an SRM
Structural design and materials	Economical and easy to apply.	Improving structural stiffness can also increase mass. Materials with lower mass density are also more expensive.	Steel: \$7-18; Grey cast iron: \$12-25; Aluminum: \$20-42; Magnesium: \$42-85	The thickness of the endplates and housing can be increased, ribs can be designed, and lighter materials can be opted for housing and end plates.
Passive vibration dampers	Economical. Various VEM grades cater to a wide range of frequency requirements.	Inefficient at a higher temperature. Ages quickly at extreme working condition.	Vibration damper: \$1-15; Vibration isolator: \$7-36; Layer dampers: \$10-35	Vibration damper between stator housing and endplates. Vibration isolators at the mounting location. Layer dampers on the end plate and housing outer surface.
Passive acoustic impedance using acoustical materials	Easy to apply. Suitable for high-frequency applications.	Could impact the thermal performance of an air-cooled motor. Higher temperature can affect the absorption coefficient.	Sound absorbers: \$1-130; Sound barriers: \$3-145	Wrapping sound absorber and barriers around the housing.
Active and semi-active noise and vibration control methods	Effective for lower frequencies.	Feedback sensors and anti-noise/vibration sources are expensive. Not suitable for mitigation of high-frequency noise.	ANC: > \$200; AVC: > \$800	Not suitable to mitigate high frequency electromagnetic noise.
Noise masking methods	Suitable for all frequency.	Customer expectations are not well-defined. Feedback sensors and speakers are costly.	> \$300	Masking noise using speakers based on driving and operating conditions.

CLD required for the 24/16 SRM. Considering the mass of the 24/16 SRM, it was assumed for cost estimation that the vibration isolators withstand at least 5 kg load at each motor mount location.

### C. PASSIVE ACOUSTIC IMPEDANCE USING ACOUSTICAL MATERIALS

Acoustical materials such as sound absorbers and sound barriers provide an excellent way to attenuate acoustic noise. Acoustical materials can be easily wrapped around the noise source. They are suitable for high-frequency applications, because they tend to get bulkier as the frequency decreases. The outer surface area of the 24/16 SRM has been considered to estimate the cost of acoustical materials. Sound barriers can be in the form of flexible acoustical foam. Opting for a two-inch thick foam to have a better absorption coefficient above 500 Hz can cost \$1-40. Sound barriers can also be fiber-based panels which are usually placed on the walls. They can be stiffer than acoustical foam. However, they can be tailored to fit the housing of the SRM. Fiber-based panels are costlier than acoustical foams because they provide a better absorption coefficient [151], [152]. A two-inch thick panel may cost \$35-130 to cover the 24/16 SRM.

Sound barriers suitable for SRMs can be in the form of mass-loaded vinyl or polyester-based panels with vinyl outer layers. Mass-loaded vinyl is generally available with a thickness of one-fourth to one-eighth of an inch, which may cost \$3-20 to enclose the 24/16 SRM. Polyester-based panels with vinyl outer layers are commonly used in civil, construction, or industrial area and can reduce the noise up to 10 dB. It may have a thickness of 1-1.5 inches and would cost \$140-145 to enclose the 24/16 SRM.

### D. ACTIVE AND SEMI-ACTIVE ACOUSTIC NOISE AND VIBRATION CONTROL METHODS

Active and semi-active control methods such as Active Noise Cancellation (ANC) and Active Vibration Control (AVC) require a feedback mechanism with multiple sensors and secondary noise/vibration sources, making them more expensive than passive methods. ANCs are effective at lower frequencies and can be applied locally or globally. The global approach is limited to frequencies typically below 300 Hz for a vehicular application because the cabin acoustic mode starts overlapping above this frequency. The local approach is limited to frequencies typically below 500 Hz because the zone of quietness shrinks as the frequency increases. AVC methods require piezoelectric, magnetostrictive, or electromagnetic actuators. This limits the working frequency of AVC methods below 1 kHz due to the response time of the actuator. ANC can be applied to an SRM to mitigate low-frequency mechanical noises, but they may not be suitable for high-frequency electromagnetic noise. In general, AVC might not be suitable to mitigate electromagnetic noises generated from high-frequency vibrations.

To estimate the cost of an ANC system for the 24/16 SRM, a TMS320C25 digital signal processor, an Analog-to-Digital (A/D) converter, a Digital-to-Analog (D/A) converter, and a reconstruction filter are considered for the control system. Besides, an engine speed measuring sensor as a reference sensor, and four 80 dB loudspeakers as anti-noise source are also considered. The cost of a TMS320C25 digital signal processor is around \$60, and four loudspeakers cost at least \$85, making the ANC system at least \$200. For an AVC system, the same control system is considered with a high-frequency range accelerometer as a reference sensor and

an 800 N magnetic actuator as an anti-vibration source. A high-frequency range accelerometer can cost at least \$100, and an 800 N magnetic actuator can cost at least \$600. Therefore, an AVC system for the 24/16 SRM may cost at least \$800, and the cost might increase multifold if multiple reference sensors and anti-vibration sources are required.

### E. NOISE MASKING METHODS

In Active Sound Design (ASD), the frequency spectrum of the noise can be altered by adding masking noise and, hence, making it sound more pleasant. It can be a good method to mitigate the annoyance associated with the electric motor noise. ASD for an electric vehicle is a new concept. Customer expectations are still not well defined, which makes it challenging to apply this method. For the 24/16 SRM, considering a similar control system as in ANC method, a high-frequency-range accelerometer as the feedback sensor, and four 80 dB loudspeakers as the noise source, the minimum cost of an ASD system can be estimated as \$300.

### X. CONCLUSION

In this paper, a review of noise and vibration reduction methods at the transmission stage have been presented and their applicability to switched reluctance motor drives has been discussed. Plenty of literature is available on the reduction of noise in SRMs at the source level, either through electromagnetic design or by current control. However, limited research is available on noise reduction at the transmission level, either for air-borne or structure-borne noise. In this paper, the structural design and materials, passive vibration dampers, acoustic impedance using acoustical material, active and semi-active noise and vibration control, and noise masking methods have been presented to mitigate acoustic noise and vibration at the transmission stage. The advantages and challenges of each method have been discussed, cost implications have been presented, and possible ways to implement them to an SRM have been presented. Improving structural design and choosing the proper material are the fundamental steps to design for acoustic noise and vibration mitigation. Passive techniques to attenuate acoustic noise and vibration, such as the application of VEMs, are suitable for a broad frequency range, and acoustical materials are suitable for high-frequency. More research is required to investigate application of VEMs and acoustical materials to SRMs, and electric motors in general. Active and semi-active control methods, such as active noise cancellation and active vibration control are suitable for noise mitigation at low frequency. Noise masking is another approach suitable to attenuate the perceived annoyance from motor noise.

### ACKNOWLEDGMENT

The authors would like to thank ANSYS for their support with Workbench software, MathWorks for their support with MATLAB software, MSC/Hexagon for their support with

ACTRAN software, and CMC Microsystems for their support with SolidWorks software.

### REFERENCES

- [1] E. Bostanci, M. Moallem, A. Parsapour, and B. Fahimi, "Opportunities and challenges of switched reluctance motor drives for electric propulsion: A comparative study," *IEEE Trans. Transport. Electrific.*, vol. 3, no. 1, pp. 58–75, Mar. 2017.
- [2] J. O. Estima and A. J. M. Cardoso, "Efficiency analysis of drive train topologies applied to electric/hybrid vehicles," *IEEE Trans. Veh. Technol.*, vol. 61, no. 3, pp. 1021–1031, Mar. 2012.
- [3] B. Bilgin, J. W. Jiang, and A. Emadi, *Switched Reluctance Motor Drives: Fundamentals to Applications*. Boca Raton, FL, USA: CRC Press, 2018.
- [4] B. Bilgin, B. Howey, A. D. Callegaro, J. Liang, M. Kordic, J. Taylor, and A. Emadi, "Making the case for switched reluctance motors for propulsion applications," *IEEE Trans. Veh. Technol.*, vol. 69, no. 7, pp. 7172–7186, May 2020.
- [5] J. W. Jiang, B. Bilgin, and A. Emadi, "Three-phase 24/16 switched reluctance machine for a hybrid electric powertrain," *IEEE Trans. Transport. Electrific.*, vol. 3, no. 1, pp. 76–85, Mar. 2017.
- [6] A. D. Callegaro, J. Liang, J. W. Jiang, B. Bilgin, and A. Emadi, "Radial force density analysis of switched reluctance machines: The source of acoustic noise," *IEEE Trans. Transport. Electrific.*, vol. 5, no. 1, pp. 93–106, Dec. 2018.
- [7] A. D. Callegaro, B. Bilgin, and A. Emadi, "Radial force shaping for acoustic noise reduction in switched reluctance machines," *IEEE Trans. Power Electron.*, vol. 34, no. 10, pp. 9866–9878, Oct. 2019.
- [8] L. M. Iversen, R. S. H. Skov, and C. Glorieux, "Measurement of noise from electrical vehicles and internal combustion engine vehicles under urban driving conditions," in *Proc. Euronoise*, Maastricht, The Netherlands, Jun. 2015, pp. 2129–2134.
- [9] *A Study on Approach Warning Systems for Hybrid Vehicle in Motor Mode*, Jpn. Standard GRB-49-10, Japan Automobile standards Internationalization Center, Feb. 2009. [Online]. Available: <https://unece.org>
- [10] Ventec. *Electric Motors vs. Traditional Diesel Engine*. Accessed: Aug. 22, 2022. [Online]. Available: <https://ventac.com>
- [11] A. Zouani and S. Hanim, "Overview of noise and vibration in automotive engines," *Int. J. Vehicle Noise Vib.*, vol. 12, no. 2, pp. 162–181, 2016.
- [12] A. Selle, A. Stefan, A. Fisher, and A. Gunther, "Engine noise components," *MTZ Worldwide*, vol. 75, pp. 44–49, Jan. 2014.
- [13] J. Florentin, F. Durieux, Y. Kuriyama, and T. Yamamoto, "Electric motor noise in a lightweight steel vehicle," SAE Tech. Paper 2011-01-1724, 2011.
- [14] M. Bösing, "Acoustic modeling of electrical drives: Noise and vibration synthesis based on force response superposition," Ph.D. dissertation, Fac. Elect. Eng. Inf. Technol., RWTH Aachen Univ., Aachen, Germany, Sep. 2013. [Online]. Available: <http://publications.rwth-aachen.de>
- [15] D. Lennström, T. Lindbom, and A. Nykänen, "Prominence of tones in electric vehicle interior noise," in *Proc. Int. Congr. Expo. Noise Control Eng.*, Sep. 2013, pp. 508–515.
- [16] D. Henderson and R. Hamernik, "Impulse noise: Critical review," *J. Acoust. Soc. Amer.*, vol. 80, no. 2, pp. 569–584, 1986.
- [17] G. Haddle and E. Skudrzyk, "The physics of flow noise," *J. Acoust. Soc. Amer.*, vol. 46, no. 1B, pp. 130–157, 1969.
- [18] M. E. Braun, S. J. Walsh, J. L. Horner, and R. Chuter, "Noise source characteristics in the ISO 362 vehicle pass-by noise test: Literature review," *Appl. Acoust.*, vol. 74, no. 11, pp. 1241–1265, 2013.
- [19] H. Van der Auweraer and K. Janssens, "A source-transfer-receiver approach to NVH engineering of hybrid/electric vehicles," SAE Tech. Paper 2012-36-0646, 2012.
- [20] W. Tong, "Motor vibration and acoustic noise," in *Mechanical Design of Electrical Motors*. Boca Raton, FL, USA: CRC Press, 2014.
- [21] G. Fang, F. P. Scalcon, D. Xiao, R. P. Vieira, H. A. Gründling, and A. Emadi, "Advanced control of switched reluctance motors (SRMs): A review on current regulation, torque control and vibration suppression," *IEEE Open J. Ind. Electron. Soc.*, vol. 2, pp. 280–301, 2021.
- [22] J. Liang, B. Howey, B. Bilgin, and A. Emadi, "Source of acoustic noise in a 12/16 external-rotor switched reluctance motor: Stator tangential vibration and rotor radial vibration," *IEEE Open J. Ind. Appl.*, vol. 1, pp. 63–73, 2020.

- [23] J. Liang, A. D. Callegaro, B. Howey, B. Bilgin, J. Dong, J. Lin, and A. Emadi, "Analytical calculation of temporal and circumferential orders of radial force density harmonics in external-rotor and internal-rotor switched reluctance machines," *IEEE Open J. Ind. Appl.*, vol. 2, pp. 70–81, 2021.
- [24] J. Liang, A. D. Callegaro, B. Bilgin, and A. Emadi, "A novel three-dimensional analytical approach for acoustic noise modeling in switched reluctance machines," *IEEE Trans. Energy Convers.*, vol. 36, no. 3, pp. 2099–2109, Jan. 2021.
- [25] I. Husain, "Minimization of torque ripple in SRM drives," *IEEE Trans. Ind. Electron.*, vol. 49, no. 1, pp. 28–39, Feb. 2002.
- [26] C. Gan, J. Wu, Q. Sun, W. Kong, H. Li, and Y. Hu, "A review on machine topologies and control techniques for low-noise switched reluctance motors in electric vehicle applications," *IEEE Access*, vol. 6, pp. 31430–31443, 2018.
- [27] Z. Zhu, X. Liu, and Z. Pan, "Analytical model for predicting maximum reduction levels of vibration and noise in switched reluctance machine by active vibration cancellation," *IEEE Trans. Energy Convers.*, vol. 26, no. 1, pp. 36–45, Mar. 2011.
- [28] J. Furqani, C. A. Wiguna, A. Chiba, O. Gundogmus, M. Elamin, and Y. Sozer, "Analytical and experimental verification of novel current waveforms for noise reduction in switched reluctance motor," in *Proc. IEEE Int. Electr. Mach. Drives Conf.*, San Diego, CA, USA, May 2019, pp. 576–583.
- [29] A. Hofmann, A. Al-Dajani, M. Bosing, and R. W. De Doncker, "Direct instantaneous force control: A method to eliminate mode-0-borne noise in switched reluctance machines," in *Proc. Int. Electr. Mach. Drives Conf.*, May 2013, pp. 1009–1016.
- [30] J.-W. Ahn, S.-J. Park, and D.-H. Lee, "Hybrid excitation of SRM for reduction of vibration and acoustic noise," *IEEE Trans. Ind. Electron.*, vol. 51, no. 2, pp. 374–380, Apr. 2004.
- [31] J. Ye, B. Bilgin, and A. Emadi, "An offline torque sharing function for torque ripple reduction in switched reluctance motor drives," *IEEE Trans. Energy Convers.*, vol. 30, no. 2, pp. 726–735, Jun. 2015.
- [32] H. Li, B. Bilgin, and A. Emadi, "An improved torque sharing function for torque ripple reduction in switched reluctance machines," *IEEE Trans. Power Electron.*, vol. 34, no. 2, pp. 1635–1644, Feb. 2019.
- [33] Z. Xia, B. Bilgin, S. Nalakath, and A. Emadi, "A new torque sharing function method for switched reluctance machines with lower current tracking error," *IEEE Trans. Ind. Electron.*, vol. 68, no. 11, pp. 10612–10622, Nov. 2021.
- [34] N. T. Shaked and R. Rabinovici, "New procedures for minimizing the torque ripple in switched reluctance motors by optimizing the phase-current profile," *IEEE Trans. Magn.*, vol. 41, no. 3, pp. 1184–1192, Mar. 2005.
- [35] Z. Xia, G. Fang, D. Xiao, A. Emadi, and B. Bilgin, "An online torque sharing function method involving current dynamics for switched reluctance motor drives," *IEEE Trans. Transport. Electrification*, vol. 9, no. 1, pp. 534–548, Mar. 2023.
- [36] N. K. Sheth and K. R. Rajagopal, "Optimum pole arcs for a switched reluctance motor for higher torque with reduced ripple," *IEEE Trans. Magn.*, vol. 39, no. 5, pp. 3214–3216, Sep. 2003.
- [37] X. Liu and Z. Q. Zhu, "Stator/rotor pole combinations and winding configurations of variable flux reluctance machines," *IEEE Trans. Ind. Appl.*, vol. 50, no. 6, pp. 3675–3684, Nov. 2014.
- [38] J. W. Lee, H. S. Kim, B. I. Kwon, and B. T. Kim, "New rotor shape design for minimum torque ripple of SRM using FEM," *IEEE Trans. Magn.*, vol. 40, no. 2, pp. 754–757, Mar. 2004.
- [39] G. Li, J. Ojeda, S. Hlioui, E. Hoang, M. Lecrivain, and M. Gabsi, "Modification in rotor pole geometry of mutually coupled switched reluctance machine for torque ripple mitigating," *IEEE Trans. Magn.*, vol. 48, no. 6, pp. 2025–2034, Jun. 2012.
- [40] Y. K. Choi, H. S. Yoon, and C. S. Koh, "Pole-shape optimization of a switched-reluctance motor for torque ripple reduction," *IEEE Trans. Magn.*, vol. 43, no. 4, pp. 1797–1800, Apr. 2007.
- [41] A. H. Isfahani and B. Fahimi, "Comparison of mechanical vibration between a double-stator switched reluctance machine and a conventional switched reluctance machine," *IEEE Trans. Magn.*, vol. 50, no. 2, pp. 293–296, Feb. 2014.
- [42] S. Das, O. Gundogmus, Y. Sozer, J. Kutz, J. Tylanda, and R. L. Wright, "Wide speed range noise and vibration mitigation in switched reluctance machines with stator pole bridges," *IEEE Trans. Power Electron.*, vol. 36, no. 8, pp. 9300–9311, Aug. 2021.
- [43] P. O. Rasmussen, J. H. Andreasen, and J. M. Pijanowski, "Structural stator spacers—A solution for noise reduction of switched reluctance motors," *IEEE Trans. Ind. Appl.*, vol. 40, no. 2, pp. 574–581, Mar. 2004.
- [44] S. M. Castano, B. Bilgin, E. Fairall, and A. Emadi, "Acoustic noise analysis of a high-speed high-power switched reluctance machine: Frame effects," *IEEE Trans. Energy Convers.*, vol. 31, no. 31, pp. 69–77, Mar. 2016.
- [45] J. Li and Y. Cho, "Investigation into reduction of vibration and acoustic noise in switched reluctance motors in radial force excitation and frame transfer function aspects," *IEEE Trans. Magn.*, vol. 45, no. 10, pp. 4664–4667, Oct. 2009.
- [46] J.-P. Hong, K.-H. Ha, and J. Lee, "Stator pole and yoke design for vibration reduction of switched reluctance motor," *IEEE Trans. Magn.*, vol. 38, no. 2, pp. 929–932, Mar. 2002.
- [47] P. Millithaler, J.-B. Dupont, M. Ouisse, É. Sadoulet-Reboul, and N. Bouhaddi, "Viscoelastic property tuning for reducing noise radiated by switched-reluctance machines," *J. Sound Vib.*, vol. 407, pp. 191–208, Oct. 2017.
- [48] D. Chung, "Materials for vibration damping," *J. Mater. Sci.*, vol. 36, no. 24, pp. 5733–5737, 2001.
- [49] T. Pritz, "Loss factor peak of viscoelastic materials: Magnitude to width relations," *J. Sound Vib.*, vol. 246, no. 2, pp. 265–280, 2001.
- [50] Z. Li, Q. Wang, A. Luo, L. Peng, P. Fu, and Y. Wang, "Improved high cycle fatigue properties of a new magnesium alloy," *Mater. Sci. Eng., A*, vol. 582, pp. 170–177, Jan. 2013.
- [51] B. R. Powell, A. A. Luo, V. Rezhets, J. J. Bommarito, and B. L. Tiwari, "Development of creep-resistant magnesium alloys for powertrain applications: Part 1 of 2," *SAE Int. J. Mater. Manuf.*, vol. 110, pp. 406–413, Jan. 2001.
- [52] N. J. Oosting, J. Hennessy, D. T. Hanner, and D. Fang, "Application of a constrained layer damping treatment to a cast aluminum V6 engine front cover," *SAE Tech. Paper 2005-01-2286*, 2005.
- [53] C. Griffen, M. Bagherpour, and S. Wanigatunga, "Damping based solution applications of powertrain components for radiated noise," *SAE Int. J. Passenger Cars-Mech. Syst.*, vol. 116, pp. 1862–1870, Jan. 2007.
- [54] J. Campbell, "Leakage defects via bubble trails in grey iron castings," *Int. J. Metalcasting*, vol. 1, no. 1, pp. 7–20, 2007.
- [55] S. Adachi, K. Horio, Y. Nakamura, K. Nakano, and A. Tanke, "Development of Toyota IZZ-FE engine," *SAE Int. J. Engines*, vol. 107, pp. 1716–1726, Jan. 1998.
- [56] L. Myagkov, K. Mahkamov, N. Chainov, and I. Makhkamova, "Advanced and conventional internal combustion engine materials," in *Alternative Fuels and Advanced Vehicle Technologies for Improved Environmental Performance*. Cambridge, U.K.: Woodhead Publishing Limited, 2014.
- [57] A. J. Dolata, J. Wiecezorek, M. Dyzia, and M. Starczewski, "Assessment of the tribological properties of aluminum matrix composites intended for cooperation with piston rings in combustion engines," *Materials*, vol. 15, no. 11, pp. 1–14, 2022.
- [58] A. Posnyk and J. Filipczyk, "Aspects of the applications of composite materials in combustion engines," *J. KONES*, vol. 20, no. 4, pp. 357–361, 2013.
- [59] T. Liu, P. Butaud, V. Placet, and M. Ouisse, "Damping behavior of plant fiber composites: A review," *Compos. Struct.*, vol. 275, no. 114392, pp. 1–14, 2021.
- [60] R. M. Crane and J. W. Gillespie Jr., "Analytical model for prediction of the damping loss factor of composite materials," *Polym. Compos.*, vol. 13, no. 3, pp. 179–190, 1992.
- [61] R. Chandra, S. Singh, and K. Gupta, "Damping studies in fiber-reinforced composites—A review," *Compos. Struct.*, vol. 46, no. 1, pp. 41–51, 1999.
- [62] R. Chandra, S. Singh, and K. Gupta, "A study of damping in fiber-reinforced composites," *J. Sound Vib.*, vol. 262, no. 3, pp. 475–496, 2003.
- [63] N. Burger, A. Laachachi, M. Ferriol, M. Lutz, V. Toniazzo, and D. Ruch, "Review of thermal conductivity in composites: Mechanisms, parameters and theory," *Prog. Polym. Sci.*, vol. 61, pp. 1–28, Jan. 2016.
- [64] L. Davis and B. Artz, "Thermal conductivity of metal-matrix composites," *J. Appl. Phys.*, vol. 77, no. 10, pp. 4954–4960, 1995.
- [65] E. Lavernia, R. Perez, and J. Zhang, "Damping behavior of discontinuously reinforced Al alloy metal-matrix composites," *Metall. Mater. Trans. A*, vol. 26, no. 11, pp. 2803–2818, 1995.
- [66] J. Kaczmar, K. Pietrzak, and W. Włosiński, "The production and application of metal matrix composite materials," *J. Mater. Process. Technol.*, vol. 106, nos. 1–3, pp. 58–67, 2000.

- [67] E. Grover and N. Lalor, "A review of low noise diesel engine design at ISVR," *J. Sound Vib.*, vol. 28, no. 3, pp. 403–431, 1973.
- [68] S. Jenkins, N. Lalor, and E. Grover, "Design aspects of low-noise diesel engines," *SAE Int. J. Engines*, vol. 82, no. 2, pp. 969–985, 1973.
- [69] H. Mahdisoozani, M. Mohsenizadeh, M. Bahiraie, A. Kasaeian, A. Daneshvar, M. Goodarzi, and M. R. Safaei, "Performance enhancement of internal combustion engines through vibration control: State of the art and challenges," *Appl. Sci.*, vol. 9, no. 3, pp. 1–30, 2019.
- [70] L. Vadmodala, A. Chowdhury, M. T. B. Tarek, S. Das, A. W. Bandarkar, O. Gundogmus, Y. Sozer, F. Venegas, and D. Colavincenzo, "Impact of damping material on vibration isolation in switched reluctance machine," in *Proc. IEEE Energy Convers. Congr. Expo.*, Detroit, MI, USA, Oct. 2020, pp. 5553–5559.
- [71] N. Saxena, P. Pradeep, G. Mathew, S. Thomas, M. Gustafsson, and S. Gustafsson, "Thermal conductivity of styrene butadiene rubber compounds with natural rubber prophylactics waste as filler," *Eur. Polym. J.*, vol. 35, no. 9, pp. 1687–1693, 1999.
- [72] S. Santhosh, V. Velmurugan, V. Paramasivam, and S. Thanikaikarasan, "Experimental investigation and comparative analysis of rubber engine mount vibration and noise characteristics," *Mater. Today, Proc.*, vol. 21, pp. 638–642, Jan. 2020.
- [73] X. Zhou, D. Yu, X. Shao, S. Zhang, and S. Wang, "Research and applications of viscoelastic vibration damping materials: A review," *Compos. Struct.*, vol. 136, pp. 460–480, Jan. 2016.
- [74] M. D. Rao, "Recent applications of viscoelastic damping for noise control in automobiles and commercial airplanes," *J. Sound Vib.*, vol. 262, no. 3, pp. 457–474, 2003.
- [75] S. Arunkumar, K. Saisankaranarayana, and K. S. Hatti, "Noise reduction at source for a vehicle using free layer damper," SAE Tech. Paper 2011-26-0067, 2011.
- [76] M. Mehrgou, R. Jonasson, A. Duret, and S. Maier, "Simulation and application of lightweight damping sandwich material for IC engines," *SAE Tech. Paper 2018-01-1565*, 2018.
- [77] N. Tandon, B. Nakra, D. Ubhe, and N. Killa, "Noise control of engine driven portable generator set," *Appl. Acoust.*, vol. 55, no. 4, pp. 307–328, 1998.
- [78] D. A. Bies, C. H. Hansen, and C. Q. Howard, "Vibration control," in *Engineering Noise Control*. Boca Raton, FL, USA: CRC Press, 2017.
- [79] A. Baz and J. Ro, "Optimum design and control of active constrained layer damping," *J. Mech. Des.*, vol. 117, pp. 135–144, Jan. 1995.
- [80] K. Wakabayashi, Y. Honda, T. Kodama, and K. Shimoyamada, "Torsional vibration damping of diesel engine with rubber damper pulley," *JSM E Int. J. Ser. C, Dyn., Control, Robot., Des. Manuf.*, vol. 38, no. 4, pp. 670–678, 1995.
- [81] J. Zhen, A. Brames, T. Williams, and C. Metzger, "Application of an elastomeric tuned mass damper for booming noise on an off-highway machine," *SAE Tech. Paper 2013-01-2010*, 2013.
- [82] P. Pereira, D. B. Reis, and C. M. Mendonca, "Transmission mount tuning using a passive mass damper-case study," SAE Tech. Paper 2013-01-2010, 2010.
- [83] S. Kopylov, Z. Chen, and M. A. Abdelkareem, "Implementation of an electromagnetic regenerative tuned mass damper in a vehicle suspension system," *IEEE Access*, vol. 8, pp. 110153–110163, 2020.
- [84] M. P. Sacks and J. C. Swallow, "Tuned mass dampers for towers and buildings," in *Proc. Struct. Eng. Natural Hazards Mitigation*, Irvine, CA, USA, Apr. 1993, pp. 640–645.
- [85] R. J. McNamara, "Tuned mass dampers for buildings," *J. Struct. Division*, vol. 103, no. 9, pp. 1785–1798, 1977.
- [86] A. Y. Tuan and G. Shang, "Vibration control in a 101-storey building using a tuned mass damper," *J. Appl. Sci. Eng.*, vol. 17, no. 2, pp. 141–156, 2014.
- [87] S. Elias and V. Matsagar, "Research developments in vibration control of structures using passive tuned mass dampers," *Annu. Rev. Control*, vol. 44, pp. 129–156, Jan. 2017.
- [88] E. R. Fitzgerald, L. D. Grandine Jr., and J. D. Ferry, "Dynamic mechanical properties of polyisobutylene," *J. Appl. Phys.*, vol. 24, no. 5, pp. 650–655, 1953.
- [89] A. M. Baz, "Characterization of material of viscoelastic properties," in *Active and Passive Vibration Damping*. Hoboken, NJ, USA: Wiley, 2018.
- [90] C. D. Johnson, "Design of passive damping systems," *J. Mech. Des.*, vol. 117, pp. 171–176, Jan. 1995.
- [91] L. Rouleau, R. Pirk, B. Plummers, and W. Desmet, "Characterization and modeling of the viscoelastic behavior of a self-adhesive rubber using dynamic mechanical analysis tests," *J. Aerosp. Technol. Manage.*, vol. 7, pp. 200–208, Jan. 2015.
- [92] J. S. A. Payne, "Other properties relevant to engineering design," in *Engineering Design With Rubber*. London, U.K.: MacLaren and Sons, 1960.
- [93] V. Janas and R. McCullough, "The effects of physical aging on the viscoelastic behavior of a thermoset polyester," *Compos. Sci. Technol.*, vol. 30, no. 2, pp. 99–118, 1987.
- [94] R. C. W. R. K. Mobley, "Noise and vibration," in *Plant Engineer's Handbook*. Oxford, U.K.: Butterworth Heinemann, 2001.
- [95] X. Tang and X. Yan, "Acoustic energy absorption properties of fibrous materials: A review," *Compos. A, Appl. Sci. Manuf.*, vol. 101, pp. 360–380, Oct. 2017.
- [96] L. Y. L. Ang, Y. K. Koh, and H. P. Lee, "Acoustic metamaterials: A potential for cabin noise control in automobiles and armored vehicles," *Int. J. Appl. Mech.*, vol. 8, no. 5, pp. 1–35, 2016.
- [97] J. Pan and Y. Gur, "Sound package design for lightweight vehicles," *SAE Tech. Paper 2015-01-2343*, 2015.
- [98] Y. Gur, J. Pan, and D. Wagner, "Sound package development for lightweight vehicle design using statistical energy analysis (SEA)," *SAE Tech. Paper 2015-01-2302*, 2015.
- [99] Y. Gur, J. Pan, J. Huber, and J. Wallace, "MMLV: NVH sound package development and full vehicle testing," *SAE Tech. Paper 2015-01-1615*, 2015.
- [100] Z. Wei, Y. Jiang, X. Tian, W. Huang, K. Zhu, and J. Pan, "Noise reduction analysis of front compartment sound package of electric vehicle based on SEA method," *SAE Tech. Paper 2021-01-1063*, 2021.
- [101] M. Niskanen, J.-P. Groby, A. Duclos, O. Dazel, J. Le Roux, N. Poulain, T. Huttunen, and T. Lähivaara, "Deterministic and statistical characterization of rigid frame porous materials from impedance tube measurements," *J. Acoust. Soc. Amer.*, vol. 142, no. 4, pp. 2407–2418, Oct. 2017.
- [102] T. Komatsu, "Improvement of the Delany-Bazley and Miki models for fibrous sound-absorbing materials," *Acoust. Sci. Technol.*, vol. 29, no. 2, pp. 121–129, 2008.
- [103] F. Fahy and D. Thompson, "Noise control," in *Fundamentals of Sound and Vibration*. Boca Raton, FL, USA: CRC Press, 2015.
- [104] F. Sun, H. Chen, J. Wu, and K. Feng, "Sound absorbing characteristics of fibrous metal materials at high temperatures," *Appl. Acoust.*, vol. 71, no. 3, pp. 221–235, Mar. 2010.
- [105] D. R. A. Christie, "Measurement of the acoustic properties of a sound absorbing material at high temperatures," *J. Sound Vib.*, vol. 46, no. 3, pp. 347–355, Jun. 1976.
- [106] P. Saha, "Sound barriers," in *Acoustic Material: Solving the Challenge of Vehicle Noise*. Warrendale, PA, USA: SAE Int., 2021.
- [107] S. R. Mahajan and P. V. Bapat, "Specialized noise control materials in the automotive industry," *Int. J. Emerg. Sci. Eng.*, vol. 2, no. 1, pp. 35–41, 2013.
- [108] D. N. May and M. M. Osman, "The performance of sound absorptive, reflective, and T-profile noise barriers in Toronto," *J. Sound Vib.*, vol. 71, no. 1, pp. 65–71, Jul. 1980.
- [109] B. Wyerman, M. Dinsmore, P. Saha, B. Baker, A. Carey, and R. Hadi, "Automotive noise and vibration control practices in the new millennium," *SAE Tech. Paper 2003-01-1589*, 2003.
- [110] G. Fraser, "Structure borne sound in motor-vehicles using statistical energy analysis," Ph.D. dissertation, Dept. Mech. Chem. Eng., Heriot-Watt Univ. Edinburgh, Edinburgh, U.K., May 1998. [Online]. Available: <https://core.ac.uk>
- [111] R. E. Wentzel and J. VanBuskirk, "A dissipative approach to vehicle sound abatement," *SAE Tech. Paper 1999-01-1668*, 1999.
- [112] Z. Mao, M. Feng, and Y. Lin, "Application of sound package material in noise reduction of motor," *Vibroeng. Proc.*, vol. 36, pp. 66–71, Mar. 2021.
- [113] F. Di Marco, R. D'Amico, and F. Ronzio, "Electric motor encapsulation design for improved NVH: A CAE-based approach," in *Proc. Int. Congr. Exh. Noise Control Eng.*, Madrid, Spain, Jun. 2019, pp. 2464–2474.
- [114] S. M. Kuo and D. R. Morgan, "Active noise control: A tutorial review," *Proc. IEEE*, vol. 87, no. 6, pp. 943–973, Jun. 1999.
- [115] J.-D. Wu and M. R. Bai, "Digital signal processor implementation of active noise control systems for broadband noise cancellation in engine exhaust systems," *Jpn. J. Appl. Phys.*, vol. 39, no. 8, pp. 4982–4986, 2000.

- [116] Y. Kajikawa, W.-S. Gan, and S. M. Kuo, "Recent advances on active noise control: Open issues and innovative applications," *APSIPA Trans. Signal Inf. Process.*, vol. 1, no. 1, pp. 1–21, 2012.
- [117] P. N. Samarasinghe, W. Zhang, and T. D. Abhayapala, "Recent advances in active noise control inside automobile cabins: Toward quieter cars," *IEEE Signal Process. Mag.*, vol. 33, no. 6, pp. 61–73, Nov. 2016.
- [118] H. Sano, T. Inoue, A. Takahashi, K. Terai, and Y. Nakamura, "Active control system for low-frequency road noise combined with an audio system," *IEEE Trans. Speech Audio Process.*, vol. 9, no. 7, pp. 755–763, Oct. 2001.
- [119] S. M. Kuo, S. Mitra, and W.-S. Gan, "Active noise control system for headphone applications," *IEEE Trans. Control Syst. Technol.*, vol. 14, no. 2, pp. 331–335, Mar. 2006.
- [120] Z. Yang, "Design of active noise control using feedback control techniques for an acoustic duct system," in *Proc. IEEE Conf. Robot., Autom. Mechatronics*, Singapore, Dec. 2004, pp. 467–472.
- [121] S. J. Elliott and P. A. Nelson, "Active noise control," *IEEE Signal Process. Mag.*, vol. 10, no. 4, pp. 12–35, Oct. 1993.
- [122] X. Kong and S. M. Kuo, "Study of causality constraint on feedforward active noise control systems," *IEEE Trans. Circuits Syst. II, Analog Digit. Signal Process.*, vol. 46, no. 2, pp. 183–186, Feb. 1999.
- [123] T. J. Sutton, S. J. Elliott, M. M. McDonald, and T. J. Saunders, "Active control of road noise inside vehicles," *Noise Control Eng. J.*, vol. 42, no. 4, pp. 137–147, 1994.
- [124] S. J. Elliott, "A review of active noise and vibration control in road vehicles," *Inst. Sound Vib. Res., Univ. Southampton, U.K., Tech. Rep.*, 981, Dec. 2008.
- [125] W. Jung, S. J. Elliott, and J. Cheer, "Local active control of road noise inside a vehicle," *Mech. Syst. Signal Process.*, vol. 121, pp. 144–157, Jan. 2019.
- [126] P. Joseph, S. Elliott, and P. Nelson, "Statistical aspects of active control in harmonic enclosed sound fields," *J. Sound Vib.*, vol. 172, no. 5, pp. 629–655, 1994.
- [127] S. J. Elliott and J. Cheer, "Modeling local active sound control with remote sensors in spatially random pressure fields," *J. Acoust. Soc. Amer.*, vol. 137, no. 4, pp. 1936–1946, 2015.
- [128] S. J. Elliott, P. Joseph, A. Bullmore, and P. A. Nelson, "Active cancellation at a point in a pure tone diffuse sound field," *J. Sound Vib.*, vol. 120, no. 1, pp. 183–189, 1988.
- [129] Y. Yu, N. G. Naganathan, and R. V. Dukkipati, "A literature review of automotive vehicle engine mounting systems," *Mechanism Mach. Theory*, vol. 36, no. 1, pp. 123–142, 2001.
- [130] D. A. Swanson, "Active engine mounts for vehicles," *SAE Tech. Paper 1993-09-01*, 1993.
- [131] T. Ushijima and S. Kumakawa, "Active engine mount with piezo-actuator for vibration control," *SAE Tech. Paper 1993-03-01*, 1993.
- [132] S. Romling, S. Vollmann, and T. Kolkhorst, "Active engine mount system in the new Audi S8," *MTZ Worldwide*, vol. 74, pp. 44–49, Jan. 2014.
- [133] C. Bohn, A. Cortabarria, V. Härtel, and K. Kowalczyk, "Active control of engine-induced vibrations in automotive vehicles using disturbance observer gain scheduling," *Control Eng. Pract.*, vol. 12, no. 8, pp. 1029–1039, Aug. 2004.
- [134] T. Ushijima, K. Takano, and T. Noguchi, "Rheological characteristics of ER fluids and their application to anti-vibration devices with control mechanism for automobiles," *SAE Tech. Paper 1988-11-01*, 1988.
- [135] J. L. Sproston, R. Stanway, E. W. Williams, and S. Rigby, "The electrorheological automotive engine mount," *J. Electrostatics*, vol. 32, no. 3, pp. 253–259, May 1994.
- [136] S. Choi, H. Song, H. Lee, S. Lim, J. Kim, and H. Choi, "Vibration control of a passenger vehicle featuring magnetorheological engine mounts," *Int. J. Vehicle Des.*, vol. 33, nos. 1–3, pp. 2–16, 2003.
- [137] X. Gao, J. Yang, J. Wu, X. Xin, Z. Li, X. Yuan, X. Shen, and S. Dong, "Piezoelectric actuators and motors: Materials, designs, and applications," *Adv. Mater. Technol.*, vol. 5, no. 1, pp. 1–26, 2020.
- [138] R. Nava, M. A. Ponce, L. Rejón, S. Viquez, and V. M. Castaño, "Response time and viscosity of electrorheological fluids," *Smart Mater. Struct.*, vol. 6, no. 1, pp. 67–75, Feb. 1997.
- [139] E. Wendt and K. W. Büsing, "A new type of hydraulic actuator using electrorheological fluids," *Int. J. Mod. Phys. B*, vol. 13, no. 14, pp. 2176–2182, Jun. 1999.
- [140] F. Jansson and O. Johansson, "A study of active engine mounts," M.S. thesis, Dept. Syst. Eng., Linköping Univ., Linköping, Sweden, Dec. 2013. [Online]. Available: <https://www.diva-portal.org>
- [141] S. MacDonald, R. Sales, J. Lanslots, M. Bodden, and T. Belschner, "Comprehensive automotive active sound design," in *Proc. Inter-Noise Noise-Con Congr. Conf.*, New Orleans, LA, USA, Nov. 2020, pp. 467–476.
- [142] M. Bodden and T. Belschner, "Comprehensive automotive active sound design—Part 1: Electric and combustion vehicles," in *Proc. Inter-Noise Noise-Con Congr. Conf.*, Melbourne, VIC, Australia, Jun. 2014, pp. 3214–3219.
- [143] *Uniform Provisions Concerning the Approval of Quiet Road Transport Vehicles With Regard to Their Reduced Audibility*, The United Nations Economic Commission for Europe (UNECE), Geneva, Switzerland, Oct. 2017. [Online]. Available: <https://unece.org>
- [144] *Acts Adopted by Bodies Created by International Agreements*, The United Nations Economic Commission for Europe (UNECE), Geneva, Switzerland, Feb. 2018. [Online]. Available: <https://unece.org>
- [145] D. Y. Gwak, K. Yoon, Y. Seong, and S. Lee, "Application of subharmonics for active sound design of electric vehicles," *J. Acoust. Soc. Amer.*, vol. 136, no. 6, pp. 391–397, 2014.
- [146] N. W. Alt and S. Jochum, "Sound design under the aspects of musical harmonic theory," *SAE Tech. Paper 2003-01-1508*, 2003.
- [147] M. Bodden, "Principles of active sound design for electric vehicles," in *Proc. Inter-Noise Noise-Con Congr. Conf.*, Hamburg, Germany, Aug. 2016, pp. 7700–7704.
- [148] M. Maunder and B. Munday, "System for augmenting the in-cabin sound of electric vehicles," *SAE Tech. Paper 2017-01-1757*, 2017.
- [149] O. Engler, M. Hofmann, R. Mikus, and T. Hirrlé, "Mercedes-Benz SLS AMG Coupé electric drive NVH development and sound design of an electric sports car," *SAE Tech. Paper 2016-06-15*, 2016.
- [150] Aearo Technologies LLC. *ISODAMP C-8000 Series, Material Summery Sheet 51*. Accessed: Dec. 21, 2022. [Online]. Available: <https://earglobal.com>
- [151] B. Y. Büyükkakinci, N. Sökmen, and H. Küçük, "Thermal conductivity and acoustic properties of natural fiber mixed polyurethane composites," *Textile Apparel*, vol. 21, no. 2, pp. 124–132, 2011.
- [152] Second Skin Audio. *Polyzorbe™ Polyester Acoustic Panels*. Accessed: Dec. 17, 2022. [Online]. Available: <https://www.secondskinaudio.com/acoustics/polyzorbe>



**ASHISH KUMAR SAHU** (Member, IEEE) received the B.E. degree (Hons.) in mechanical engineering from the Bhilai Institute of Technology, Durg, India, in 2006, and the M.Tech. degree in mechanical engineering from the Indian Institute of Technology Kharagpur, Kharagpur, India, in 2008. He is currently pursuing the Ph.D. degree in mechanical engineering with the McMaster Automotive Resource Center, McMaster University, Hamilton, ON, Canada.

From 2008 to 2010, he was an Assistant Manager with Tata Motors Ltd., Jamshedpur, India, where his main responsibility was automotive component durability testing. From 2010 to 2019, he was a Lead Engineer with Mahindra & Mahindra, Chennai, India, where his main responsibility was virtually validating automotive components for durability. Since 2020, he has been with Dr. A. Emadi's Research Group, McMaster Automotive Resource Center, McMaster University. He has authored or coauthored nine journals and conference papers. His research interests include electromagnetic motor design, automotive body design, structural durability, and acoustic noise and vibration.





**ALI EMADI** (Fellow, IEEE) received the B.S. and M.S. degrees (Hons.) in electrical engineering from the Sharif University of Technology, Tehran, Iran, in 1995 and 1997, respectively, and the Ph.D. degree in electrical engineering from Texas A&M University, College Station, TX, USA, in 2000. He is currently the Canada Excellence Research Chair Laureate with McMaster University, Hamilton, ON, Canada. He is also the NSERC/FCA Industrial Research Chair in electrified power-

trains and a Tier I Canada Research Chair in transportation electrification and smart mobility. Before joining McMaster University, he was the Harris Perlstein Endowed Chair Professor of engineering and the Director of the Electric Power and Power Electronics Center and Grainger Laboratories, Illinois Institute of Technology, Chicago, where he established research and teaching facilities, as well as courses in power electronics, motor drives, and vehicular power systems. He was the Founder, Chairman, and President of Hybrid Electric Vehicle Technologies, Inc. (HEVT)—a university spin-off company of Illinois Technology. He is also the President and Chief Executive Officer of Enedym Inc. and Menlolab Inc.—two McMaster University spin-off companies. He is the principal author/coauthor of over 700 journals and conference papers, as well as several books, including *Vehicular Electric Power Systems* (2003), *Energy Efficient Electric Motors* (2004), *Uninterruptible Power Supplies and Active Filters* (2004), *Modern Electric, Hybrid Electric, and Fuel Cell Vehicles* (2nd edition, 2009), and *Integrated Power Electronic Converters and Digital Control* (2009). He was the Inaugural General Chair of the 2012 IEEE Transportation Electrification Conference and Expo (ITEC) and has chaired several IEEE and SAE conferences in the areas of vehicle power and propulsion. He is the Editor of the *Handbook of Automotive Power Electronics and Motor Drives* (2005) and *Advanced Electric Drive Vehicles* (2014). He is also the Co-Editor

of *Switched Reluctance Motor Drives* (2018). He was the founding Editor-in-Chief of IEEE TRANSACTIONS ON TRANSPORTATION ELECTRIFICATION, from 2014 to 2020.



**BERKER BILGIN** (Senior Member, IEEE) received the Ph.D. degree in electrical engineering from Illinois Institute of Technology, Chicago, IL, USA, in 2011, and the M.B.A. degree from DeGroote School of Business, McMaster University, Hamilton, ON, Canada, in 2018. He is currently an Assistant Professor with the Department of Electrical and Computer Engineering (ECE), McMaster University. He is also the Co-Founder and the Vice President of

engineering with Enedym Inc., Hamilton, which is a spin-off company of McMaster University, specializing in electric machines, electric motor drives (EMDs), advanced controls and software, and virtual engineering. He has authored or coauthored 127 journals and conference papers and three book chapters. He is the Lead Editor and the author of the textbook titled *SRM Drives: Fundamentals to Applications*. He is the principal inventor/co-inventor of ten patents and pending patent applications. His current research interests include electric machines, switched reluctance motor (SRM) drives, acoustic noise and vibration analysis and reduction, power electronics, and EMDs. He was elected as the General Chair of the 2016 IEEE Transportation Electrification Conference and Expo (ITEC). He serves as an Associate Editor for IEEE TRANSACTIONS ON TRANSPORTATION ELECTRIFICATION.

• • •